ACS APPLIED MATERIALS & INTERFACES

Forum Article

www.acsami.org

Synthesis of Novel Gold Mesoflowers as SERS Tags for Immunoassay with Improved Sensitivity

Chunyuan Song, Linghua Min, Ni Zhou, Yanjun Yang, Shao Su, Wei Huang, and Lianhui Wang*

Key Lab Organic Electronics & Information Displays (KLOEID), and Institute of Advanced Materials (IAM), Nanjing University of Posts & Telecommunications, Nanjing 210023, China

Supporting Information

ABSTRACT: A new class of flowerlike gold mesostructure in high yield is successfully synthesized through a facile one-step route using ascorbic acid as a reducing agent of gold salt with cetyltrimethylammonium chloride (CTAC) as surfactant. The as-prepared Au particles have spherical profiles with an averaged diameter of 770 ± 50 nm, but showing a highly rough surface consisting of many irregular and randomly arranged protrusions. The Au mesoflowers exhibit strong surface-enhanced effects and near-infrared absorption which were utilized in the design of efficient surface-enhanced Raman scattering (SERS) tags as immunosensors for immunoassay with improved sensitivity. The experimental results indicate that a good linear relationship is found between the peak intensity at 1071 cm^{-1} and the logarithm of H-IgG concentration in the range between 1 ng/mL and 1 fg/mL, and the limit of detection (LOD) is 1 fg/mL.

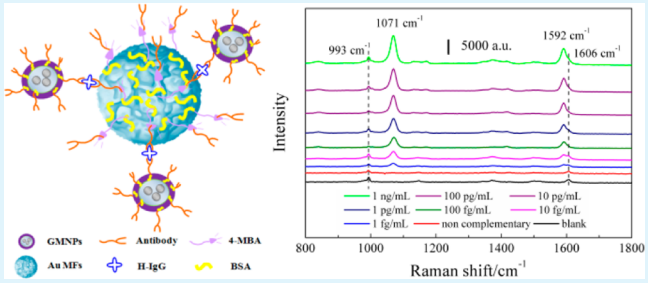

KEYWORDS: *flowerlike gold mesostructures, surface-enhanced Raman scattering, immunoassay, SERS tags*

1. INTRODUCTION

An immunoassay is considered as a powerful tool for disease diagnosis, drug discovery, environmental monitoring, and food safety.[1−3] Comparing with traditional detection methods, e.g., fluorescence-based detection systems or enzyme-linked immunosorbent assay (ELISA) with some technical drawbacks like poor signal-to-noise ratio and low limit of detection,[4−6] surface enhanced Raman scattering (SERS)-based detection has been expected to be a promising and significant technique for highly sensitive immunoassay, since SERS possesses the unique features with ultrahigh sensitivity, antiphotobleaching and multiplex detection capability.[7,8]

Typically, SERS-based immunoassay utilizes a standard protocol of sandwich structure, including immuno-substrate (i.e., supporting substrates), SERS-active immunosensor (i.e., SERS tags) and the target protein. It is well-known that a highly sensitive SERS-based immunoassay is critically related to the SERS response capability of the SERS tags. Therefore, a variety of SERS tags consisting of nanostructures such as various shapes of gold nanoparticles,[9−16] Au−Ag core−shell,[17,18] nanohollows[19,20] and aggregates[21] have been developed and tested until now as SERS-active biosensors. Nevertheless, it is still highly desirable for ultrasensitive assays to design brighter SERS tags that combine facile and versatile synthesis with high stability. In recent years, experimental measurements[22−24] and theoretical calculations[25−27] have shown that stronger enhancement of the electromagnetic field generates near the surface of the complex Au nanostructures (e.g., dendrites, multipods, and highly branched hyperpods such as flowerlike particles) which exhibit strong plasmon resonances close to the NIR window of biological transparency and, particularly, high electromagnetic field localized at their protrusions (so-called "hot spots"). Therefore, their synthesis and applications as SERS tags are of interest to SERS-based bioassays. However, the synthesis of flower-shaped colloid is a fairly recent development, relying on a one-pot process[10,12,28] or multiple-step method[29,30] (i.e., the seed-mediated growth method) by using specific capping agents to induce anisotropic growth.

Unlike previous studies on synthesis of highly branched dendritic flowerlike nanostructures, herein we report a simple one-step synthesis by using ascorbic acid as a reducing agent of gold salt in CTAC surfactant to prepare a new class of monodisperse flowerlike gold mesostructure in high yield. The as-synthesized gold mesoflowers with highly irregular and rough surface exhibit strong SERS activity and NIR absorption, indicating potential applications in the design of efficient SERS tags. A preliminary study of SERS-based immunoassay demonstrates that using such immunosensor and combining with SERS-active Au coated magnetic nanoparticles as supporting substrates, a trace concentration (1 fg/mL) of Human IgG can be detected. Because of the high sensitivity and

Special Issue: Materials for Theranostics

Received: April 30, 2014
Accepted: July 24, 2014
Published: August 4, 2014

good selectivity, the proposed Au MFs SERS sensor might have potential application for SERS-based biodetections.

2. EXPERIMENTAL SECTION

2.1. Materials. Cetyltrimethylammonium chloride (CTAC, ≥96%) and hydrogen tetrachloroaurate(III) trihydrate ($HAuCl_4 \cdot 3H_2O$, 99.99%) were purchased from Alfa Aesar. 4-Mercaptobenzoic acid (4-MBA, 99%), tetrakis(hydroxymethyl)phosphonium chloride (THPC, 80% aqueous solution), *N*-hydroxysuccinimide (NHS), and 1-ethyl-3-(3-(dimethylamino)propyl) carbodiimide (EDC) were obtained from Sigma-Aldrich. Ammonium hydroxide (25.0−28.0%), L-ascorbic acid (AA, ≥ 99.7%) and ethanol (≥99.7%) were bought from Sinopharm Chemical Reagent Co., Ltd. 3-Aminopropyltriethoxysilane (APTES, 98%) and teraethyl orthosilicate (TEOS) were purchased from Aladdin. Goat antihuman IgG (2 mg/mL), human IgG (H-IgG), and mouse IgG (M-IgG) (10 mg/mL) were provided by Beijing Biosynthesis Biotechnology Co., Ltd. Bovine serum albumin (BSA) was purchased from Biosharp. Ultrapure Millipore water (18.2 MΩ cm^{-1}) was used as the solvent throughout. Borate buffer solution (BBS, 2 mM, pH 9) was served as the buffer solution.

2.2. Synthesis of Flowerlike Gold Mesostructures. A new class of flowerlike gold mesostructures (Au MFs) was developed by using AA as a reducing agent of gold salt in CTAC surfactant. Specifically, 10 mL of 10 mM $HAuCl_4$ aqueous solution was mixed with 100 mL of 200 mM CTAC aqueous solution under vigorous stirring. Then 5 mL of 300 mM AA aqueous solution was added into the mixture and stirred vigorously for 2 min. The mixture was then left undisturbed at 15 °C to grow Au MFs. After 3 h, the as-synthesized colloidal suspension was centrifuged at 900 rpm for 5 min to remove the excess reactants. The precipitates were collected and washed three times. Finally, these particles were dried and redispersed with BBS to 10 mg/mL.

2.3. Preparation of SERS Immuno-Au MFs as SERS Tags. 4-MBA (1 mM, in ethanol solution) was served as the Raman reporter and slowly added into 5 mL of colloidal gold under vigorous stirring and the resultant mixture was allowed to react overnight. After centrifugal purification (900 rpm for 5 min), the particles were modified with 4-MBA by S-metal covalent bond, leaving carboxyl groups outside. These carboxylate-terminations were used to obtain a stable immobilization of the proteins by covalent bonding via the esterification of NHS (372 μL of 100 mM) with EDC (150 μL of 100 mM). Briefly, goat antihuman IgG (200 μL, 2 mg/mL) was added into the NHS-activated Au MFs and incubated at 4 °C for 6 h. The products were further blocked by BSA (500 μL, 3% in BBS) for 1 h, followed by centrifugal purification for three times. Finally, the SERS immuno-Au MFs (4-MBA-labeled Au MFs immunosensor) were obtained by redispersing the precipitates into 4 mL BBS.

2.4. Preparation of SERS Immuno-GMNPs as Supporting Substrates. *Synthesis of Gold-Coated Magnetic Nanoparticles.* Magnetic nanoparticles (MNPs), Fe_3O_4, were synthesized by chemical codeposition of $FeCl_2$ and $FeCl_3$ in aqueous solution, following the synthesis method proposed by Kang et al.[31] The as-synthesized MNPs colloid was finally dried in a vacuum oven at 70 °C and then the powder was dispersed to 10 mg/mL by water. The gold-coated magnetic nanoparticles (GMNPs) were synthesized by three steps described in the Supporting Information (Figure S1). First, the Fe_3O_4@SiO_2 nanoparticles were synthesized by hydrolysis of TEOS in an alkaline environment, followed by an aminosilylation of APTES. Second, Au seeds (3−5 nm) were absorbed onto the aminated Fe_3O_4@SiO_2 nanoparticles to form Fe_3O_4@SiO_2@Au seeds structure. In the final step, the Au seeds on the surface of Fe_3O_4@SiO_2 grew to be a compact but rough gold shell on the Fe_3O_4@SiO_2. After purification, 3 mL of Fe_3O_4@SiO_2@Au particles (GMNPs) in BBS was obtained.

Modification of the GMNPs with Antibodies. One milliliter of 5-fold diluted GMNPs was mixed with antibodies (200 μL of 2 mg/mL goat antihuman IgG) and incubated at 4 °C for more than 12 h to modify the antibodies onto the GMNPs. The antibody-modified GMNPs were then blocked by BSA (500 μL, 3%). Finally, 3 mL of SERS immuno-GMNPs was obtained by magnetic separation and redispersion with BBS.

2.5. Sandwich Immunoassay. Two hundred microliters of SERS tags were added into a tube and mixed together homogeneously with 150 μL of SERS immuno-GMNPs at 4 °C, followed by adding the target antigen (H-IgG). After being incubated for 3 h under shaking, the mixture was separated by a magnet and washed three times by BBS. Finally, the purified composites were dispersed in 100 μL of water for SERS measurements. The schematic illustration of the protocol for sandwich immunoassay can be found in Figure 1.

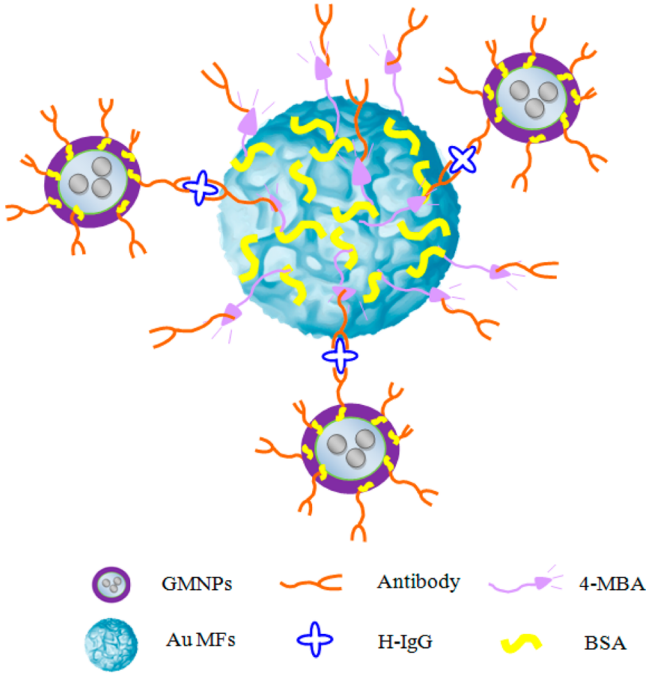

Figure 1. Schematic illustration of the protocol of sandwich immunoassay.

For SERS detections, 5 aliquots of 10 μL final immune products were dropped onto silica wafer (1 cm × 1 cm) respectively, and below each sample point there was placed a cylindrical magnet (diameter ~1.5 mm, length ~10 mm) to magnetically concentrate the immune products into a small spot with diameter less than 1 mm, followed by several SERS detections (power 30 mW, acquisition time 5 s) performed in the spot.

2.6. Instrumentation. The UV−vis−NIR spectrophotometer (UV-3600, Shimadzu, Japan) was used to monitor the absorption properties of the colloids. Transmission electron microscopy (TEM) (HT7700, Hitachi, Japan) and field emission scanning electron microscopy (FESEM) (S-4800, Hitachi, Japan) were utilized to characterize the morphology and distribution of particles. The SERS spectra were recorded by a HRC-10HT Raman Analyzer (Enwave Optronics Inc.), with a 785 nm excitation wavelength and a ~100 μm laser spot.

3. RESULTS AND DISCUSSION

3.1. Synthesis of SERS-Active Gold Mesoflowers. The proposed novel SERS-active Au MFs were synthesized by a facile and one-step route conducted at 15 °C, using AA as a reducing agent of gold salt in CTAC surfactant. Figure 2a shows the morphology of as-synthesized gold mesoflowers. According to the FESEM image, it is clear that almost all the Au particles have a spherical profiles with the averaged diameter of 770 ± 50 nm, but showing highly rough surfaces consisting of many irregular and randomly arranged protrusions. Such

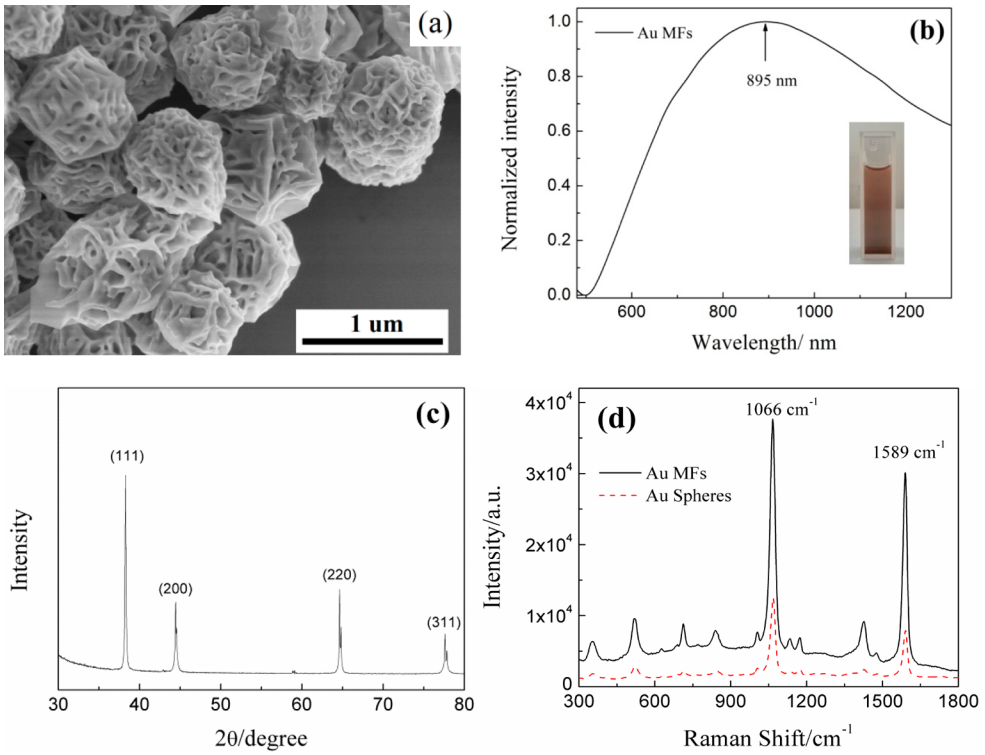

Figure 2. Characterizations of Au MFs. (a) FESEM image, (b) optical property, (c) XRD pattern, (d) SERS spectra of 4-MBA absorbed on the as-synthesized gold mesoflowers (Au MFs) and spherical gold particles (Au Spheres).

flowerlike gold crystals in high yield can be called gold mesoflowers.

The color of the colloid is brown and the optical property of the as-synthesized Au MFs is shown in Figure 2b. The Au MFs show an absorption band from ~600 nm to NIR, with a surface plasmon resonance (SPR) peak centered at 895 nm, which illustrates that the resonance condition can be well-established when stimulated by the 785 nm incident laser beam.

The crystal structure and the phase composition of the as-synthesized mesostructures were characterized by XRD. Figure 2c shows a typical XRD pattern of the Au MFs, in which four peaks can be observed, corresponding to diffractions from the (111), (200), (220), and (311) planes of the face-centered-cubic (fcc) phase.[32,33] This indicates that the flowerlike gold mesostructures are well-crystallized.

The SERS activity of Au MFs was characterized by using 4-MBA as Raman molecule. Briefly, 100 μL of 4-fold concentrated Au colloid was mixed together with 10 μL of 1 mM 4-MBA. Then 10 μL mixture was spotted onto a glass slide. After natural air drying, the sample with an approximate diameter of 3 mm was scanned by Raman Analyzer with 20 mW excitation power and a collection time of 30 s. The solid curve in Figure 2d shows the averaged SERS spectrum of six scans at different positions in the sample spot. The characteristic Raman peak of 4-MBA at 1589 and 1066 cm^{-1}, which are assigned to ν_{8a} and ν_{12} aromatic ring vibrations, can be seen clearly. The SERS spectrum of 4-MBA exhibited some peak shifts compared to its normal Raman spectrum,[34] which are induced by the interaction of Au MFs with 4-MBA. Using the same synthesis parameters but higher growth temperature (>25 °C), spherical gold particles with averaged diameter 500 ± 50 nm were also synthesized. Comparing with the SERS spectrum of 4-MBA detected from these spherical gold particles (dashed curve shown in Figure 2d), it can be concluded that the as-synthesized Au MFs possess stronger SERS activity, because many "hot spots" distribute on their rough surface with many randomly arranged protrusions and lots of gaps between these protrusions.

The stability of the Au MFs is characterized by absorption spectra, as shown in the Supporting Information (Figure S2). The red curve is the absorption spectrum of the as-synthesized Au MFs stored at 4 °C for 1 month. Comparing with the absorption spectrum of the fresh Au MFs (black curve), only a very slight peak shift appears, which indicates that the colloids have good stability.

3.2. Design and Characterization of SERS Immuno-Au MFs. The SERS tags were designed basing on the novel SERS-active Au MFs by two steps, i.e., labeling Raman reporters and immobilizing complementary antibodies of the target antigen. Herein, 4-MBA molecules were served as both the SERS reporters and the conjugation agent for attaching antibodies onto the Au MFs, with their thiol groups linking to the surfaces of Au MFs in a monolayer and the EDC and NHS activated carboxyl groups covalently bonding with the amino groups of antibodies.[35] Considering the traditional strategy that both the reporter molecules and proteins are immobilized onto the limited surface area of SERS particles, such modified design can provide as many surface areas as possible for Raman molecules anchoring and further capturing more antibodies onto the particles through the amidation reaction between carboxyl and amino groups. These SERS tags are expected to exhibit better response capability, resulting in an improved detection sensitivity.

The maximum load capacity of 4-MBA on the Au MFs was investigated by mixing 25, 50, 75, 100, and 150 μL of 1 mM 4-MBA with 1 mL of Au colloids, respectively, followed by centrifugal purification. The normalized absorption spectra of the five samples are shown in Figure 3a. The different 4-MBA-

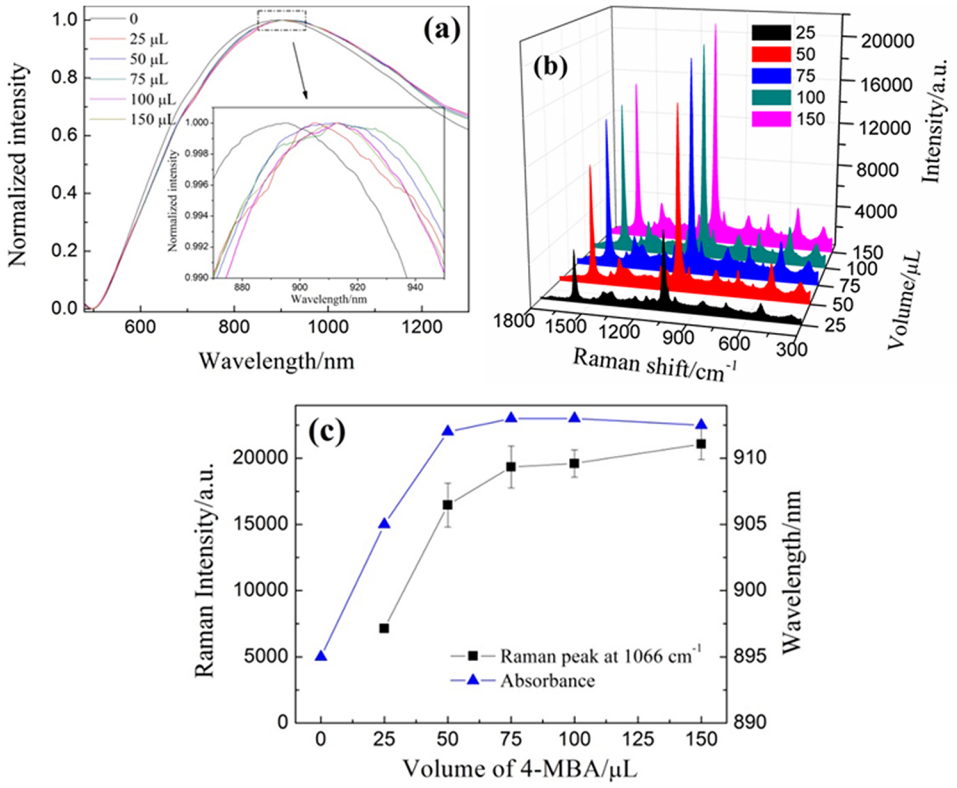

Figure 3. (a) Absorption and (b) SERS characterization of the 4-MBA-labeled Au MFs by mixing the Au MFs with 0, 25, 50, 75, 100, and 150 μL of 1 mM 4-MBA, respectively; (c) changes of absorption peak and intensity of the characteristic SERS peak of 4-MBA at 1066 cm^{-1} along with the increasing volume of 4-MBA added into the Au MFs colloid, respectively.

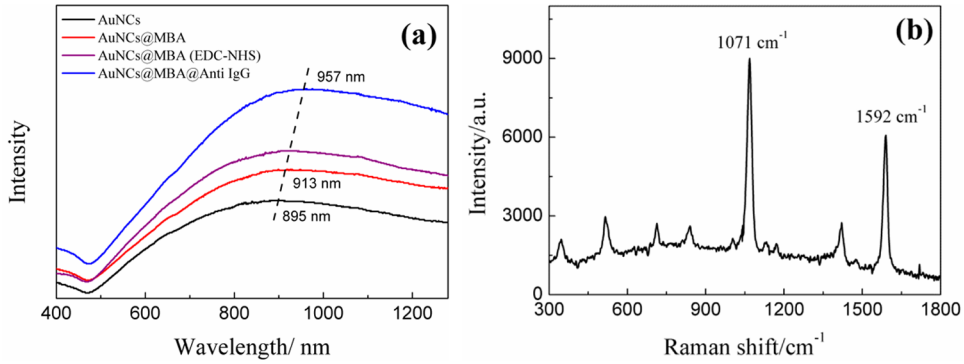

Figure 4. Characterization of immuno-Au MFs. (a) Absorption spectra of Au MFs collected after each preparation step of immuno-Au MFs. (b) SERS characterization of immuno-Au MFs (10 mW excitation power, 60 s acquisition time).

labeled Au MFs show similar absorption spectra to the one of as-synthesized Au MFs, but with slightly peak shift as illustrated in Figure 3a. The SPR peak of Au MFs redshifts 10 to 905 nm when reacted with 25 μL of 4-MBA, followed by another 7 nm redshift when adding 50 μL of 4-MBA, which means that the original surface ion (CTA^+) on the Au MFs were replaced by reporter molecules, causing changes of the dielectric constant of microenvironment around the particles.[36] After that, although the added volume of Raman reporters was increasing (75, 100, and 150 μL), the SPR peak hardly moves and stabilizes near 913 nm, which indicates that the replace of surface ions almost ceased and the surface coverage of 4-MBA on the Au MFs was maximum. The efficiency of Raman reporter labeling on the particles was also characterized by SERS measurements (10 mW excitation power, 60 s acquisition time). According to the averaged SERS spectra shown in Figure 3b, the SERS signal shows a variation similarly to the absorption spectrum (Figure 3c). Take the characteristic peak at 1066 cm^{-1} for example, along with the increasing volume of 4-MBA added into Au MFs, the signal intensity increases from 7143 ± 247 to 16473 ± 1663 au, and then showing a very small change around 20 000 au. On the basis of the above investigation, a typical procedure of Raman reporter labeling could be defined, i.e., adding 100 μL of 1 mM 4-MBA into 1 mL as-synthesized Au colloid.

Further, the 4-MBA-labeled Au MFs with carboxyl groups outside were activated by EDC and NHS, forming amine-reactive O-acylisourea intermediates to reacted with the amine groups on the antibodies, as a result yielding conjugates of the two molecules joined by stable amide bonds.[37] The activation process causes very slight changes of the SPR peak. In contrast, the following coupling of antibodies onto the Au MFs results in a significant redshift of 44 to 957 nm (Figure 4a), which

dx.doi.org/10.1021/am502636h | ACS Appl. Mater. Interfaces 2014, 6, 21842−21850

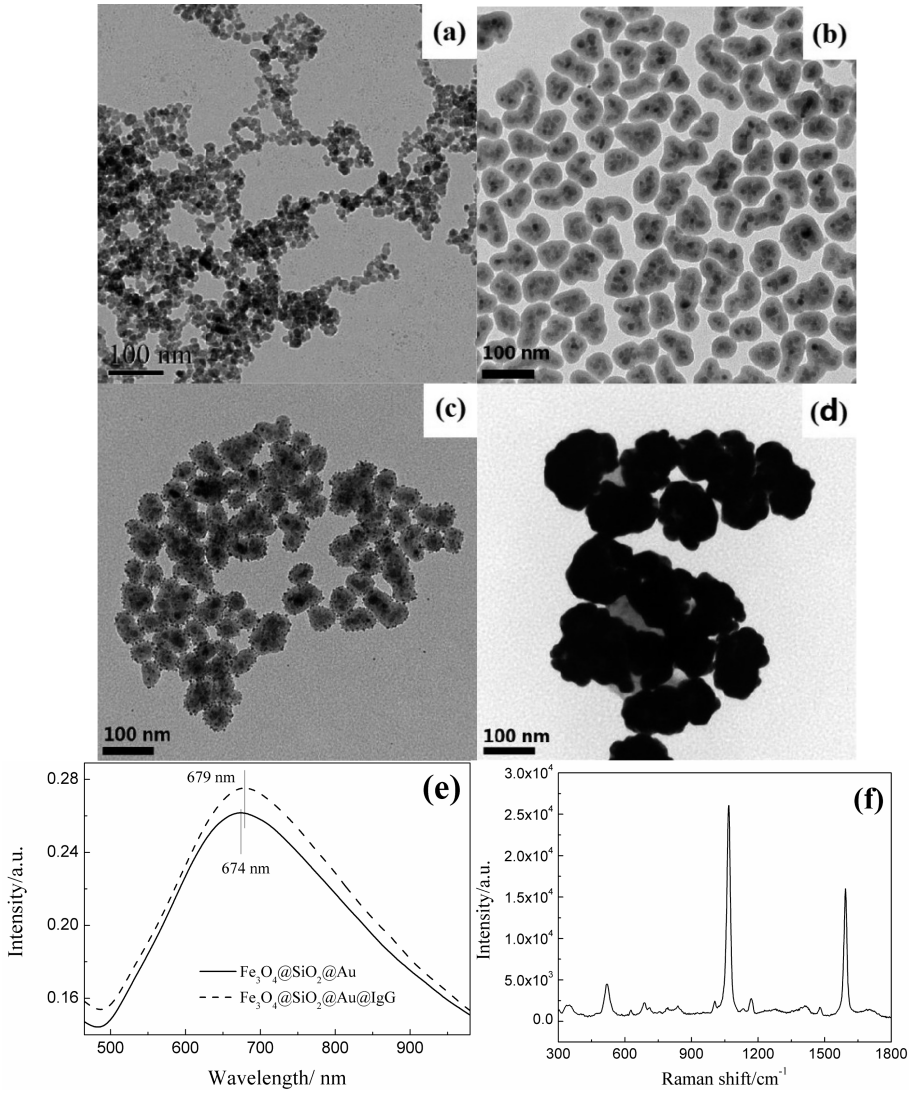

Figure 5. TEM images of (a) Fe_3O_4 nanoparticles, (b) Fe_3O_4@SiO_2 core−shell structures, (c) Fe_3O_4@SiO_2@Au seeds, (d) Fe_3O_4@SiO_2@Au shell. (e) Absorption spectra of GMNPs before (solid) and after (dashed) immobilization of antibodies. (f) SERS spectrum of 4-MBA absorbed on the Fe_3O_4@SiO_2@Au particles (30 mW excitation power, 5 s acquisition time).

indicates that antibodies are immobilized onto the 4-MBA-labeled Au MFs successfully.[38] The SERS activity of immuno-Au MFs was characterized and the averaged SERS signal is shown in Figure 4b, which demonstrates that the obtained SERS immuno-Au MFs possess strong surface-enhanced effects. Note that because the COOH group of 4-MBA underwent covalent conjugation with antibodies, the two characteristic SERS peaks of 4-MBA shift to 1071 and 1592 cm^{-1}, respectively, after antibody modifications.

The capture efficiency of the antibodies onto the Au MFs is investigated. We conducted a simple experiment in which the goat antihuman IgG antibodies were replaced by FITC-labeled goat antihuman IgG antibodies and allowed to anchor onto the Au MFs modified with 0, 25, and 100 μL of 1 mM 4-MBA (denoted as Au MFs_{-0}, Au MFs_{-25}, and Au MFs_{-100}, respectively). After centrifugal purification, the supernatants of the three samples (denoted as residual solutions) were collected respectively and examined by fluorescence spectroscopy (RF-5301PC, Shimadzu, Japan). The fluorescence intensities at the 519 nm FITC peak are 287.91, 277.38, and 258.60 counts for the residual solutions of Au MFs_{-0}, Au MFs_{-25}, and Au MFs_{-100}, respectively (shown in the Supporting Information, Figure S3). As a reference, the unused FITC-labeled antibody solution diluted to the same volume of the other samples shows a fluorescence intensity of 310.41 counts. Thus, assuming each antibody carries the same amount of FITC molecules, the amount ratio κ of antibodies immobilized on Au MFs_{-0}, Au MFs_{-25}, and Au MFs_{-100} (denoted as $\kappa_{AuMFs-0}$, $\kappa_{AuMFs-25}$, and $\kappa_{AuMFs-100}$, respectively) can be estimated using the fluorescence signal of the residual solutions as follows

$$\kappa_{AuMFs-0} = \frac{I - I_{AuMFs-0}}{I} = 7.25\% \quad (1)$$

$$\kappa_{AuMFs-25} = \frac{I - I_{AuMFs-25}}{I} = 10.64\% \quad (2)$$

$$\kappa_{AuMFs-100} = \frac{I - I_{AuMFs-100}}{I} = 16.70\% \quad (3)$$

where I, $I_{AuMFs-0}$, $I_{AuMFs-25}$, and $I_{AuMFs-100}$ represent the 519 nm peak intensities detected from unused FITC-labeled goat antihuman IgG solution, and the residual solutions of Au MFs_{-0}, Au MFs_{-25}, and Au MFs_{-100}, respectively. These

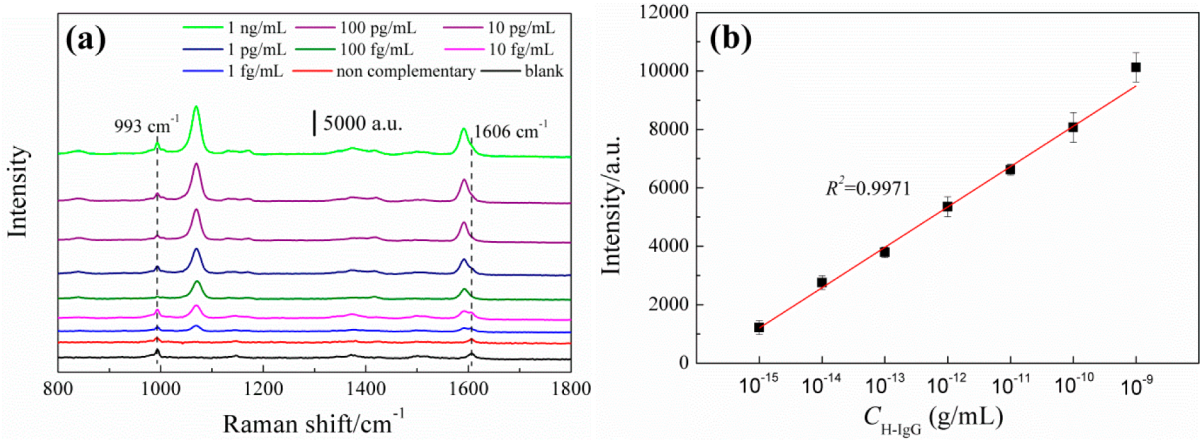

Figure 6. (a) SERS spectra obtained with different concentrations of target H-IgG (1 ng/mL to 1 fg/mL) in the sandwich immunoassay, noncomplementary, and blank, respectively. (b) Linear fitting of the peak intensities at 1071 cm^{-1} as a function of the logarithm of H-IgG concentration. Error bars indicate the standard deviation obtained from eight measurements.

calculations indicate that the amount of antibodies anchored onto the Au MFs_{-100} is 1.57 times and 2.30 higher in relative to those on Au MFs_{-25} and Au MFs_{-0}, respectively, which confirms that the more 4-MBA molecules are immobilized on the Au MFs, a higher adsorption rate for antihuman IgGs captured on the particles through the amidation reaction between carboxyl and amino groups can be obtained.

3.3. Characterization of SERS Immuno-GMNPs. Figure 5a shows the morphology of MNPs with an averaged diameter of ~13 nm. These nanoparticles with high saturation magnetization (65.98 emu/g) exhibit superparamagnetic property,[39] as shown in the Supporting Information (Figure S4). As we know, the greatest advantage of superparamagnetic nanoparticles is related to their fast and facile separation by implementing an external magnetic field.[40,41] These MNPs were then coated with a thin layer of silica shell for further amination with APTES. Figure 5b shows the TEM image of silica-coated MNPs. Statistical results indicate that in each core−shell structure there are 11 ± 1 MNPs and the shell thickness is approximated as 11.3 ± 0.2 nm. The morphology of Au seeds absorbed Fe_3O_4@SiO_2 is shown in Figure 5c. It can be clearly seen that many small Au seeds (diameter 3−5 nm) are captured onto the surface of SiO_2 shell, serving as seeds for further Au shell growth. The final Au shell with rough surface can be found distinctly from Figure 5d. The optical property of Au shell was characterized and Figure 5e illustrates that the SPR peak of the Fe_3O_4@SiO_2@Au is centered at 674 nm. According to the SERS spectrum of 1×10^{-4} M 4-MBA detected from GMNPs substrate shown in Figure 5f, we can conclude that these GMNPs exhibit strong surface enhancement effect and can be served as good SERS substrates combining with magnetic performance. The immobilization of antibodies onto the GMNPs was also characterized by the UV−vis−NIR spectrophotometer. As the dashed curve in Figure 5e shows, the SPR peak of Au shell redshifts 5 nm, which indicates that the antibodies anchoring on the Au shell and SERS-active immuno-GMNPs were obtained.

3.4. SERS-Based Immunoassay. By using the SERS immuno-Au MFs and SERS immuno-GMNPs, we performed sandwich immunoassays to detect 1 ng/mL H-IgG, as the solid line shows in the Supporting Information (Figure S4). As a control, the other immunoassay conducted with the same protocol except that the Au MFs SERS tags were replaced by the spherical gold particle SERS tags, as the dashed line shown in Supporting Information (Figure S5). The experimental results illustrate that an improved sensitivity can be obtain by using Au MFs SERS tags. It should be pointed out that the density of SERS tags used in the detection should be considered.[42] The preliminary result indicates that if more SERS tags are used, fewer GMNPs can be found in each immune composite, which may result in a decrease in the "hot spots" on the composites formed between the Au MFs and GMNPs, and affect the efficiency of magnetic separation. If more immuno-GMNPs are used in the immunoassay, after magnetic separation there are too many GMNPs in the immune products which can obstruct the irradiation of laser onto the SERS tags. Both the two conditions can reduce the detection sensitivity.

Concentrations of H-IgG ranged from 1 ng/mL to 1 fg/mL were prepared and the concentration-dependent SERS spectra were detected. Besides, M-IgG (1 ng/mL) was selected for unspecific immunoassays, and a blank control was carried out by performing the sandwich immunoassay without adding any antigens. Figure 6a illustrates the averaged SERS spectra of the concentration-dependent detections, the non complementary and blank control, respectively. It is observed that the intensity of the 1071 and 1592 cm^{-1} peaks from 4-MBA decrease with the reducing human IgG concentration. As shown in Figure 6b, a good linear relationship is found between the peak intensity at 1071 cm^{-1} and the logarithm of H-IgG concentration in the range between 1 fg/mL and 1 ng/mL. To the non-complemental and blank controls shown in Figure 6a, because no sandwich structured composites were formed, the two characteristic peaks of 4-MBA disappear from their SERS spectra. It should be pointed out that another two peaks at 993 and 1606 cm^{-1} are attributed to the surfactant on the GMNPs instead of 4-MBA. The immunoassay results demonstrate that the proposed SERS immuno-Au MFs possess high sensitivity and specificity, by using Au MFs SERS immuno-sensor and combining with the immuno-GMNPs as the immuno-substrate, an ultrasensitive and specific immunoassay was performed and the detection limit of H-IgG is as low as 1 fg/mL, which is better than the most reported SERS immunoassay based on the sandwich structure protocol.[17,18,32,38,43−46] Such high detection sensitivity might be due to the proposed brighter SERS tags and additional enormous SERS "hot spots" emerging among

Au MFs and Fe_3O_4@SiO_2@Au rough surface formed between the junctions of the sandwich structured composites.[38,47−49]

Those results presented above were confirmed by the TEM images of the sandwich structured composites in the immune products. Specifically, five aliquots of 10 μL composites from 1 ng/mL, 10 fg/mL, and 1 fg/mL H-IgG, the noncomplementary, and blank control, were transferred onto Cu grids, respectively, followed by TEM characterization. The distributions of the sandwich structured composites in each sample can be seen in Figure 7. Figure 7a shows the TEM image of the immunoassay with 1 ng/mL H-IgG, from which we can find many aggregates. By checking all the aggregates showing in the image, the composites including GMNPs (smaller particles) and Au MFs (bigger particles) are marked with square frame, and the other aggregates are assembled by GMNPs without any Au MFs. A typical composite is shown in Figure 7b, which is an enlarged picture of the aggregate marked in blue in Figure 7a. Similarly, Figure 7c−f illustrate the distributions of the immune products with 10 fg/mL and 1 fg/mL H-IgG, respectively, and g and h correspond to the blank and noncomplemental controls, respectively. According to the magnified pictures b, d, and f shown in Figure 7, many "hot spots" are estimated to be formed on the aggregates. Further statistical results of Figure 7a, c, and e indicate that there are about 131, 25, and 16 Au MFs per 2000 μm^2 respectively, corresponding to about 514, 98, and 63 Au MFs being illuminated by incident laser beam (laser spot ~100 μm). This result is consistent with the change of SERS signals mentioned above. Besides, according to the TEM images shown in Figure 7g, h, almost no such composites including Au MFs can be found from the blank and noncomplementary immune products. The TEM characterizations also demonstrate that those novel immuno-Au MFs have good biological specificity and high sensitivity.

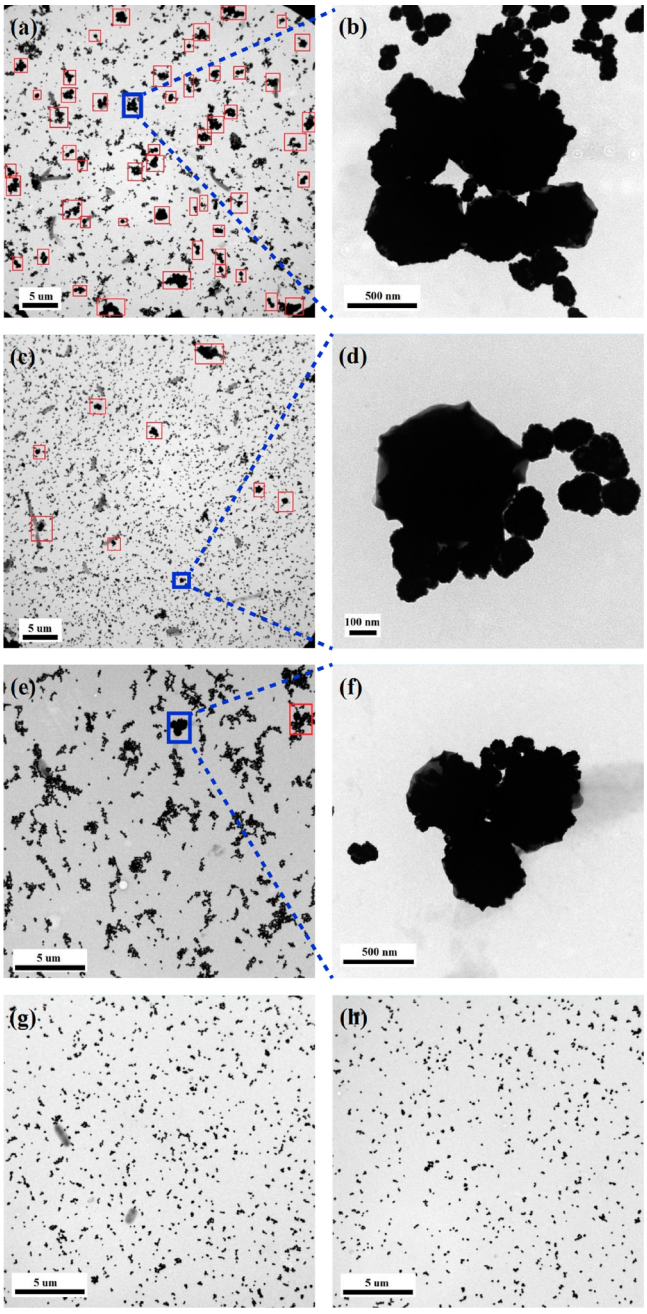

Figure 7. TEM images of immune composites obtained with different concentrations of target H-IgG in the sandwich immunoassay: (a−f) 1 ng/mL, 10 fg/mL, and 1 fg/mL H-IgG, respectively, with each magnified image of the composites marked with blue frame; (g) blank, and (h) noncomplementary.

4. CONCLUSIONS

In this study, a new class of gold mesoflowers was synthesized in high yield by a facile and one-step route conducted at 15 °C, using ascorbic acid as a reducing agent of gold salt in CTAC surfactant. The Au mesoflowers with an average size about 770 nm possess an irregular rough surface and a NIR absorption, which exhibited strong SERS effects. The Au MFs could also be developed into SERS immuno-sensors by linking Raman molecules and specific antibodies of the target. The effectiveness of these immuno-Au MFs for protein detection was then demonstrated by a sandwich protocol immunoassay using SERS-active Fe_3O_4@SiO_2@Au as supporting substrates. A good linear relationship is found between the peak intensity at 1071 cm^{-1} and the logarithm of H-IgG concentration in the range between 1 fg/mL and 1 ng/mL. The limit of detection (LOD) is 1 fg/mL. Such ultrasensitive SERS-based immunoassay possesses potential applications for disease diagnosis, drug discovery, environmental monitoring, and food safety. And the proposed novel flowerlike gold mesostructures are expected to be developed into various SERS biosensors for detection of different targets.

■ ASSOCIATED CONTENT

Ⓢ Supporting Information

The procedure of synthesis of gold-coated magnetic nanoparticles, sketch map of synthesis of gold-coated magnetic nanoparticles (Figure S1); absorption spectra of the fresh Au MFs and the Au MFs stored at 4 °C for 1 month (Figure S2);fluorescence spectra of the residual solutions of Au MFs_{-0}, Au MFs_{-25}, and Au MFs_{-100}, respectively (Figure S3); the magnetic hysteresis curve of Fe_3O_4 nanoparticles (Figure S4); and SERS spectra obtained from sandwich immunoassay with same protocol but different SERS tags, Au MFs and Au spheres (Figure S5). This material is available free of charge via the Internet at http://pubs.acs.org.

■ AUTHOR INFORMATION

Corresponding Author

*E-mail: iamlhwang@njupt.edu.cn. Tel: +86 25 85866333.

Author Contributions

The manuscript was written through contributions of all authors. All authors have given approval to the final version of the manuscript.

Notes

The authors declare no competing financial interest.

■ ACKNOWLEDGMENTS

This work was financially supported by the National Key Basic Research Program of China (2012CB933301), National Natural Science Foundation of China (61302027, 21305070), Natural Science Foundation of Jiangsu Province of China (BK20130871, BK20130861), Natural Science Fund for Colleges and Universities in Jiangsu Province (13KJB140009), Program for Changjiang Scholars and Innovative Research Team in University (IRT1148), Sci-tech Support Plan of Jiangsu Province (BE2014719), a project funded by the Priority Academic Program Development of Jiangsu Higher Education Institutions (PAPD), and the Open Research Fund of State Key Laboratory of Bioelectronics, Southeast University.

■ REFERENCES

(1) Wang, Y. R.; Li, P. W.; Majkova, Z.; Bever, C. R. S.; Kim, H. J.; Zhang, Q.; Dechant, J. E.; Gee, S. J.; Hammock, B. D. Isolation of Alpaca Anti-Idiotypic Heavy-Chain Single-Domain Antibody for the Aflatoxin Immunoassay. *Anal. Chem.* **2013**, *85*, 8298−8303.

(2) Jin, M. J.; Zhu, G. N.; Jin, R. Y.; Liu, S. Y.; Shao, H.; Jin, F.; Guo, Y. R.; Wang, J. A Sensitive Chemiluminescent Enzyme Immunoassay for Carbofuran Residue in Vegetable, Fruit and Environmental Samples. *Food Agric. Immunol.* **2013**, *24*, 345−356.

(3) Wang, Y. M. C.; Jawa, V.; Ma, M. Immunogenicity and PK/PD Evaluation in Biotherapeutic Drug Development: Scientific Considerations for Bioanalytical Methods and Data Analysis. *Bioanalysis* **2014**, *6*, 79−87.

(4) Wang, Y.; Yan, B.; Chen, L. SERS Tags: Novel Optical Nanoprobes for Bioanalysis. *Chem. Rev.* **2012**, *113*, 1391−1428.

(5) Rosi, N. L.; Mirkin, C. A. Nanostructures in Biodiagnostics. *Chem. Rev.* **2005**, *105*, 1547−1562.

(6) Chon, H.; Lim, C.; Ha, S. M.; Ahn, Y.; Lee, E. K.; Chang, S. I.; Seong, G. H.; Choo, J. On-Chip Immunoassay Using Surface-Enhanced Raman Scattering of Hollow Gold Nanospheres. *Anal. Chem.* **2010**, *82*, 5290−5295.

(7) Jun, B. H.; Kim, J. H.; Park, H.; Kim, J. S.; Yu, K. N.; Lee, S. M.; Choi, H.; Kwak, S. Y.; Kim, Y. K.; Jeong, D. H.; Cho, M. H.; Lee, Y. S. Surface-Enhanced Raman Spectroscopic-Encoded Beads for Multiplex Immunoassay. *J. Comb. Chem.* **2007**, *9*, 237−244.

(8) Vendrell, M.; Maiti, K. K.; Dhaliwal, K.; Chang, Y.-T. Surface-Enhanced Raman Scattering in Cancer Detection and Imaging. *Trends Biotechnol.* **2013**, *31*, 249−257.

(9) Luo, Z. H.; Li, W. T.; Lu, D. L.; Chen, K.; He, Q. G.; Han, H. Y.; Zou, M. Q. A SERS-Based Immunoassay for Porcine Circovirus Type 2 Using Multi-Branched Gold Nanoparticles. *Microchim. Acta* **2013**, *180*, 1501−1507.

(10) Sanda, B.; Dumitrita, R.; Adela, P.; Lucian, B.-T.; Simion, A. Flower-shaped Gold Nanoparticles: Synthesis, Characterization and Their Application as SERS-Active Tags inside Living Cells. *Nanotechnology* **2011**, *22*, 055702.

(11) Rodriguez-Lorenzo, L.; Krpetic, Z.; Barbosa, S.; Alvarez-Puebla, R. A.; Liz-Marzan, L. M.; Prior, I. A.; Brust, M. Intracellular Mapping with SERS-Encoded Gold Nanostars. *Integr. Biol.* **2011**, *3*, 922−926.

(12) Xie, J.; Zhang, Q.; Lee, J. Y.; Wang, D. I. C. The Synthesis of SERS-Active Gold Nanoflower Tags for In Vivo Applications. *ACS Nano* **2008**, *2*, 2473−2480.

(13) Lu, G.; Li, H.; Liusman, C.; Yin, Z.; Wu, S.; Zhang, H. Surface Enhanced Raman Scattering of Ag or Au Nanoparticle-Decorated Reduced Graphene Oxide for Detection of Aromatic Molecules. *Chem. Sci.* **2011**, *2*, 1817−1821.

(14) Lu, G.; Li, H.; Wu, S.; Chen, P.; Zhang, H. High-Density Metallic Nanogaps Fabricated on Solid Substrates Used for Surface Enhanced Raman Scattering. *Nanoscale* **2012**, *4*, 860−863.

(15) Lu, G.; Li, H.; Zhang, H. Nanoparticle-Coated PDMS Elastomers for Enhancement of Raman Scattering. *Chem. Commun.* **2011**, *47*, 8560−8562.

(16) Lu, G.; Li, H.; Zhang, H. Gold-Nanoparticle-Embedded Polydimethylsiloxane Elastomers for Highly Sensitive Raman Detection. *Small* **2012**, *8*, 1336−1340.

(17) Wu, L.; Wang, Z. Y.; Zong, S. F.; Huang, Z.; Zhang, P. Y.; Cui, Y. P. A SERS-Based Immunoassay with Highly Increased Sensitivity Using Gold/Silver Core-Shell Nanorods. *Biosens. Bioelectron.* **2012**, *38*, 94−99.

(18) Cui, Y.; Ren, B.; Yao, J.-L.; Gu, R.-A.; Tian, Z.-Q. Synthesis of AgcoreAushell Bimetallic Nanoparticles for Immunoassay Based on Surface-Enhanced Raman Spectroscopy. *J. Phys. Chem. B* **2006**, *110*, 4002−4006.

(19) Lee, S.; Chon, H.; Lee, J.; Ko, J.; Chung, B. H.; Lim, D. W.; Choo, J. Rapid and Sensitive Phenotypic Marker Detection on Breast Cancer Cells Using Surface-Enhanced Raman Scattering (SERS) Imaging. *Biosens. Bioelectron.* **2014**, *51*, 238−243.

(20) Chon, H.; Lee, S.; Son, S. W.; Oh, C. H.; Choo, J. Highly Sensitive Immunoassay of Lung Cancer Marker Carcinoembryonic Antigen Using Surface-Enhanced Raman Scattering of Hallow Gold Nanospheres. *Anal. Chem.* **2009**, *81*, 3029−3034.

(21) Song, C. Y.; Wang, Z. Y.; Yang, J.; Zhang, R. H.; Cui, Y. P. Preparation of 2-Mercaptobenzothiazole-Labeled Immuno-Au Aggregates for SERS-Based Immunoassay. *Colloids Surf., B* **2010**, *81*, 285−288.

(22) Jia, W.; Li, J.; Jiang, L. Synthesis of Highly Branched Gold Nanodendrites with a Narrow Size Distribution and Tunable NIR and SERS Using a Multiamine Surfactant. *ACS Appl. Mater. Interfaces* **2013**, *5*, 6886−6892.

(23) You, H.; Ji, Y.; Wang, L.; Yang, S.; Yang, Z.; Fang, J.; Song, X.; Ding, B. Interface Synthesis of Gold Mesocrystals with Highly Roughened Surfaces for Surface-Enhanced Raman Spectroscopy. *J. Mater. Chem.* **2012**, *22*, 1998−2006.

(24) Rodriguez-Lorenzo, L.; Alvarez-Puebla, R. A.; de Abajo, F. J. G.; Liz-Marzan, L. M. Surface Enhanced Raman Scattering Using Star-Shaped Gold Colloidal Nanoparticles. *J. Phys. Chem. C* **2010**, *114*, 7336−7340.

(25) Hao, E.; Bailey, R. C.; Schatz, G. C.; Hupp, J. T.; Li, S. Synthesis and Optical Properties of "Branched" Gold Nanocrystals. *Nano Lett.* **2004**, *4*, 327−330.

(26) Bakr, O. M.; Wunsch, B. H.; Stellacci, F. High-Yield Synthesis of Multi-Branched Urchin-Like Gold Nanoparticles. *Chem. Mater.* **2006**, *18*, 3297−3301.

(27) Kumar, P. S.; Pastoriza-Santos, I.; Rodriguez-Gonzalez, B.; de Abajo, F. J. G.; Liz-Marzán, L. M. High-Yield Synthesis and Optical Response of Gold Nanostars. *Nanotechnology* **2008**, *19*, 015606.

(28) Nhung, T. T.; Bu, Y.; Lee, S.-W. Facile Synthesis of Chitosan-Mediated Gold Nanoflowers as Surface-Enhanced Raman Scattering (SERS) Substrates. *J. Cryst. Growth* **2012**, *373*, 132−137.

(29) Sanchez-Gaytan, B. L.; Qian, Z.; Hastings, S. P.; Reca, M. L.; Fakhraai, Z.; Park, S.-J. Controlling the Topography and Surface Plasmon Resonance of Gold Nanoshells by a Templated Surfactant-Assisted Seed Growth Method. *J. Phys. Chem. C* **2013**, *117*, 8916−8923.

(30) Sajanlal, P. R.; Pradeep, T. Mesoflowers: A New Class of Highly Efficient Surface-Enhanced Raman Active and Infrared-Absorbing Materials. *Nano Res.* **2009**, *2*, 306−320.

(31) Kang, K.; Choi, J.; Nam, J. H.; Lee, S. C.; Kim, K. J.; Lee, S.-W.; Chang, J. H. Preparation and Characterization of Chemically Functionalized Silica-Coated Magnetic Nanoparticles as a DNA Separator. *J. Phys. Chem. B* **2008**, *113*, 536−543.

(32) Yanxiao, L.; Zhanfang, M. Facile Fabrication of Truncated Octahedral Au Nanoparticles and Its Application for Ultrasensitive

Surface Enhanced Raman Scattering Immunosensing. *Nanotechnology* **2013**, *24*, 275605.
(33) Xie, J.; Lee, J. Y.; Wang, D. I. Seedless, Surfactantless, High-Yield Synthesis of Branched Gold Nanocrystals in HEPES Buffer Solution. *Chem. Mater.* **2007**, *19*, 2823−2830.
(34) Michota, A.; Bukowska, J. Surface-Enhanced Raman Scattering (SERS) of 4-Mercaptobenzoic Acid on Silver and Gold Substrates. *J. Raman Spectrosc.* **2003**, *34*, 21−25.
(35) Yang, J.; Wang, Z. Y.; Tan, X. B.; Li, J.; Song, C. Y.; Zhang, R. H.; Cui, Y. P. A Straightforward Route to The Synthesis of a Surface-Enhanced Raman Scattering Probe for Targeting Transferrin Receptor-Overexpressed Cells. *Nanotechnology* **2010**, *21*, 345101.
(36) Kelly, K. L.; Coronado, E.; Zhao, L. L.; Schatz, G. C. The Optical Properties of Metal Nanoparticles: The Influence of Size, Shape, and Dielectric Environment. *J. Phys. Chem. B* **2002**, *107*, 668−677.
(37) Liang, Y.; Gong, J.-L.; Huang, Y.; Zheng, Y.; Jiang, J.-H.; Shen, G.-L.; Yu, R.-Q. Biocompatible Core-Shell Nanoparticle-Based Surface-Enhanced Raman Scattering Probes for Detection of DNA Related to HIV Gene Using Silica-Coated Magnetic Nanoparticles as Separation Tools. *Talanta* **2007**, *72*, 443−449.
(38) Song, C. Y.; Wang, Z. Y.; Zhang, R. H.; Yang, J.; Tan, X. B.; Cui, Y. P. Highly Sensitive Immunoassay Based on Raman Reporter-Labeled Immuno-Au Aggregates and SERS-Active Immune Substrate. *Biosens. Bioelectron.* **2009**, *25*, 826−831.
(39) Li, L.; Yang, Y.; Ding, J.; Xue, J. Synthesis of Magnetite Nanooctahedra and Their Magnetic Field-Induced Two-/Three-Dimensional Superstructure. *Chem. Mater.* **2010**, *22*, 3183−3191.
(40) Chen, L.; Hong, W.; Guo, Z. N.; Sa, Y.; Wang, X.; Jung, Y. M.; Zhao, B. Magnetic Assistance Highly Sensitive Protein Assay Based on Surface-Enhanced Resonance Raman Scattering. *J. Colloid Interface Sci.* **2012**, *368*, 282−286.
(41) Wang, Y.; Ravindranath, S.; Irudayaraj, J. Separation and Detection of Multiple Pathogens in a Food Matrix by Magnetic SERS Nanoprobes. *Anal. Bioanal. Chem.* **2011**, *399*, 1271−1278.
(42) Qu, L.; Xu, J.; Tan, X.; Liu, Z.; Xu, L.; Peng, R. Dual-Aptamer Modification Generates a Unique Interface for Highly Sensitive and Specific Electrochemical Detection of Tumor Cells. *ACS Appl. Mater. Interfaces* **2014**, *6*, 7309−15.
(43) Shen, A.; Chen, L.; Xie, W.; Hu, J.; Zeng, A.; Richards, R.; Hu, J. Triplex Au−Ag−C Core−Shell Nanoparticles as a Novel Raman Label. *Adv. Funct. Mater.* **2010**, *20*, 969−975.
(44) Zong, S. F.; Wang, Z. Y.; Zhang, R. H.; Wang, C. L.; Xu, S. H.; Cui, Y. P. A Multiplex and Straightforward Aqueous Phase Immunoassay Protocol through The Combination of SERS-Fluorescence Dual Mode Nanoprobes and Magnetic Nanobeads. *Biosens. Bioelectron.* **2013**, *41*, 745−751.
(45) Pei, Y. W.; Wang, Z. Y.; Zong, S. F.; Cui, Y. P. Highly Sensitive SERS-Based Immunoassay with Simultaneous Utilization of Self-Assembled Substrates of Gold Nanostars and Aggregates of Gold nanostars. *J. Mater. Chem. B* **2013**, *1*, 3992−3998.
(46) Ni, J.; Lipert, R. J.; Dawson, G. B.; Porter, M. D. Immunoassay Readout Method Using Extrinsic Raman Labels Adsorbed on Immunogold Colloids. *Anal. Chem.* **1999**, *71*, 4903−4908.
(47) Chen, S. A.; Yuan, Y. X.; Yao, J. L.; Han, S. Y.; Gu, R. A. Magnetic Separation and Immunoassay of Multi-antigen Based on Surface Enhanced Raman Spectroscopy. *Chem. Commun.* **2011**, *47*, 4225−4227.
(48) Han, X. X.; Kitahama, Y.; Itoh, T.; Wang, C. X.; Zhao, B.; Ozaki, Y. Protein-Mediated Sandwich Strategy for Surface-Enhanced Raman Scattering: Application to Versatile Protein Detection. *Anal. Chem.* **2009**, *81*, 3350−3355.
(49) Song, C. Y.; Wang, Z. Y.; Yang, J.; Zhang, R. H.; Cui, Y. P. Effects of Solid Substrate on The SERS-Based Immunoassay: a Comparative Study. *J. Raman Spectrosc.* **2011**, *42*, 313−318.